

Photon-assisted tunneling in electron pumps

M. Covington, Mark W. Keller, R. L. Kautz and John M. Martinis
National Institute of Standards and Technology, Boulder, CO 80303

We measure photon-assisted tunneling in 4- and 6-junction electron pumps at photon frequencies up to 60 GHz. We determine the microwave voltage at the pumps using noise thermometry. The standard theory of leakage in the electron pump, modified to include photon-assisted tunneling, describes our experiments well. From this test of theory we argue that, in the absence of external microwaves, photon-assisted tunneling driven by $1/f$ noise is an important error mechanism in electron pumps.

PACS #'s: 73.23.Hk, 85.30.Wx

Tunneling through a junction with capacitance C_0 is suppressed if the single-electron charging energy $e^2/2C_0$ is larger than the thermal energy $k_B T$. Single-electron tunneling (SET) devices exploit this energy barrier to detect and/or manipulate individual electrons [1]. One such device, the electron pump [2], consists of a chain of metal islands separated by tunnel junctions, with each island coupled capacitively to a gate electrode (see Fig. 1a). One electron is transferred through the device by pulsing the gate voltages to lower the energy barrier and allow tunneling at each junction in sequence. Although electron transfer with an error of only 1 part in 10^8 has been demonstrated in a 7-junction pump [3, 4], this is not nearly as low as theory predicts. Recent studies [4, 5] show that theory agrees with experiment at temperatures above 100 mK, where errors due to unwanted thermally-activated tunneling dominate. However, between 100 mK and 30 mK the experimental error rate is constant, while theory predicts it should drop by orders of magnitude. Simple explanations of this discrepancy in terms of uncertainty in pump parameters or heating can be excluded because all parameters, including the electron temperature in the pump, were measured [4]. Therefore, the discrepancy implies the presence of an important error process that is not included in the theory.

It has been well established that the electromagnetic environment seen by a junction influences tunneling rates [6]. Standard SET theory includes the effects of zero-point fluctuations and temperature in the environment, and has been used to explain the stringent requirements for observing SET effects in single junctions. In multi-junction devices, zero-point fluctuations and temperature (if appropriate filters are used [7]) typically have negligible effects, and thus the environment is commonly not included in theoretical analyses of these devices. However, an environment containing a time-varying voltage source with spectral components at frequencies corresponding to the charging energy (typically ~ 10 GHz) will significantly increase tunneling rates because it will generate photons of sufficient energy to overcome the charging energy barrier. Based on this picture and the experimental results described above, photon-assisted tunneling (PAT)

has been proposed as the source of the excess errors in electron pumps [4]. There have been many previous studies of PAT [8], including some concerned specifically with SET devices, both experimental [9] and theoretical [10]. Previous SET studies considered systems of one or two junctions, usually biased with a voltage, for which the current due to PAT appears on top of a background current $\sim 10^{-12}$ A due to other tunneling processes. Here we report studies of multi-junction pumps with no voltage bias and without the gate voltage pulses used to pump electrons, for which the background tunneling rates correspond to currents $\sim 10^{-19}$ A or less. This low background allows us to investigate the regime of very rare errors that is relevant for proposed applications of SET technology, including a new fundamental capacitance standard based on accurate counting of electrons [11]. We compare measurements of pumps in the presence of a well-characterized microwave source with an extension of standard SET theory that includes PAT. Based on our results, we propose that (in the absence of applied microwaves) an important error mechanism at low temperature is PAT driven by $1/f$ noise at microwave frequencies.

A general formalism for treating a multi-junction device in an environment containing an arbitrary voltage source has been described by Martinis and Nahum [7]. For a transition involving a particular junction j that takes the device between initial and final states differing in electrostatic energy by ΔE_j , the tunneling rate is

$$\Gamma_e(\Delta E_j) = \int_{-\infty}^{\infty} d\varepsilon P(\varepsilon) \Gamma_0(\Delta E_j - \varepsilon), \quad (1)$$

where $\Gamma_0(\Delta E_j)$ is the rate when environmental effects are neglected [12] and $P(\varepsilon)$ is the probability for the emission ($\varepsilon > 0$) or absorption ($\varepsilon < 0$) of energy ε by the device. $P(\varepsilon)$ depends on the environmental impedance $Z_e(\omega)$ at frequencies up to $\omega \sim (e^2/2C_0)/\hbar$ [6]. When $Z_e(\omega) \ll h/e^2$, $\varepsilon < 0$, $|\varepsilon| > k_B T$, and in the limit of a weak source (single-photon processes only), $P(\varepsilon)$ is given by

$$P(\varepsilon) = \frac{\pi e^2 S_v(|\varepsilon|/\hbar)}{h \varepsilon^2}, \quad (2)$$

where $S_V(\omega)$ is the spectral density of the voltage across the junction [7]. Thus, for any environment that produces a voltage $V(t)$ across the junction, the probability of the junction absorbing an energy $\hbar\omega$ is determined by $S_V(\omega)$. If $\hbar\omega$ is larger than ΔE_j for a given transition, this energy absorption will cause $\Gamma_e(\Delta E_j)$ to be significantly larger than $\Gamma_0(\Delta E_j)$ for that transition. This process corresponds to PAT.

In our experiments, we apply a voltage $V(t) = V_0 \sin(\omega t)$, corresponding to $S_V(\omega) \propto \delta(\omega - \omega_0)$, to an electron pump through a coplanar waveguide and termination resistor as shown in Fig. 1b. The termination is composed of a Au-Pd layer that provides the requisite 50 Ω resistance and overlying Au stripes that reduce heating by increasing the volume. The Au stripes also reduce the thermal resistance between neighboring Au-Pd regions to ensure uniform heating. The lumped circuit model in Fig. 1a is adequate since the distance between the voltage tap and the pump is small (less than $\lambda/7$ for $f < 60$ GHz) and the capacitance to ground between the tap and the pump is small. The pumps have Al junctions and are fabricated on fused silica substrates using optical and electron-beam lithography designs described previously [13].

An accurate measurement of the microwave voltage at the pump is essential for comparison with theory. The power in the termination P_{term} differs from the known output power of the microwave generator P_{out} by an attenuation factor A that depends on frequency. We determine $P_{term} = P_{out}/A$ at each frequency by performing an ac/dc substitution measurement in the termination. That is, we find P_{term} by measuring heating in the termination at ac using noise thermometry calibrated at dc. The heating is described by $T_e^5 = T_{ph}^5 + (P_{out}/A)/\Sigma\Theta$, where T_e is the electron temperature, T_{ph} is the lattice temperature, Σ describes the electron-phonon coupling strength in the material, and Θ is the termination volume [14]. We use a SQUID amplifier to measure the Johnson noise, and thus T_e , in the termination [15]. Separate temperature calibrations determine T_{ph} [16], and the termination dimensions give $\Theta = 4.1 \times 10^4 \mu\text{m}^3$. From dc measurements where A is known, we find $\Sigma = 1.4 \text{ nW}/(\mu\text{m}^3 \cdot \text{K}^5)$. We determine A at each frequency by fitting the heating equation given above to the measured T_e as a function of P_{out} at that frequency. We find good fits to T_e vs. P_{out}/A (an example is shown in Fig. 2), demonstrating that our model accurately describes heating in the termination. Thus for any microwave generator power and frequency we can determine the actual power in the termination and, accounting for voltage division, the amplitude of the sinusoidal voltage across the pump V_0 . Figure 2 shows that heating is negligible over the range of P_{term} (arrows) used to investigate PAT.

We characterize and operate the pumps using techniques described previously [3, 13]. For simplicity when comparing with theory, we measure leakage in the

static hold mode rather than errors in the pumping mode where the gates are pulsed. A leakage event causes the charge on the stray capacitance $C_s \approx 22$ pF of the 100 $\mu\text{m} \times 100 \mu\text{m}$ island between the pump and the electrometer to change by $\pm e$, and this change is detected by the electrometer [3]. The leakage rate γ is the total number of such events (in either direction) per unit time. Before measuring γ , we adjust the dc gate voltages to minimize the error rate while pumping with $V_0 = 0$ [13]. This compensates for the random background charges that polarize the islands of the pump and fluctuate over time scales of hours.

Typical PAT data from 4- and 6-junction electron pumps are shown in Figures 3 and 4, respectively. Two observations regarding these measurements can be made immediately. First, in the main plot of each figure, $\chi(f)$ at constant V_0 is flat at low frequency and increases sharply at a threshold frequency ~ 40 GHz. This behavior is characteristic of PAT. The fine structure in these curves is generally not repeatable and is probably due to small variations in the background charges during the measurement. Second, in the inset of each figure, $\chi(V_0)$ at $f = 60$ GHz is flat for small V_0 and approaches $\gamma \propto V_0^4$ at larger V_0 . Although the threshold frequencies are close to the expected values (see below), we must consider the possible contribution of harmonics of the applied frequency. We have repeated our measurements with a 0.3 m length of stainless steel coax inserted into the microwave line at room temperature. This coax has a frequency-dependent attenuation such that it acts as a low-pass filter. With the coax in place, we observe that the power required to produce a given leakage rate is larger by an amount equal to the attenuation of the coax at the fundamental frequency. Thus, the fundamental, rather than harmonics, is responsible for the observed effect.

Our theoretical calculations are based on a circuit model in which all junctions have capacitance C_j and resistance R_j , and all other capacitance is represented by a capacitor C_{gnd} from each island to ground [5, 17]. This model accurately describes the nonuniform distribution of V_0 along the pump due to capacitive division. We determine R_j from current-voltage measurements and C_j and C_{gnd} from “electron box” measurements that give the charging energy of each junction [4]. In order to include processes involving multiple photons, which are not described by Eq. (1), we use a modified version of the procedure used in the absence of radiation [5]. The modification consists of replacing the rate $\Gamma_0^{(m)}(\Delta E)$ for m -th order cotunneling in the absence of microwaves with

$$\Gamma^{(m)} = \sum_{n=-\infty}^{\infty} J_n^2(e\bar{V}_j/\hbar\omega) \Gamma_0^{(m)}(\Delta E - n\hbar\omega), \quad (3)$$

where J_n is the n th-order Bessel function, ω is the microwave angular frequency, and \bar{V}_j is the average of the microwave voltage amplitudes across the m junctions involved in the process. Equation (3) exactly reproduces

results derived previously for single-junction processes [10] and gives an estimate for higher-order processes that agrees with the result of [7] for $m = 2$ in the appropriate limit. The leakage rate γ is found by considering all possible tunneling sequences that result in one electron passing through the whole pump [5], and we compare $\gamma + \gamma_b$, where γ_b is the background leakage rate measured in the absence of microwaves, with the measured $\chi(f)$ and $\chi(V_0)$. Although all parameters needed for the calculations are measured, the combined uncertainty in the theoretical predictions is large. Therefore, we fit calculations based on Eq. (3) to the experimental data using two scaling factors, β_C for capacitance and β_V for microwave voltage. That is, T_e, f, R_j , and C_{gnd}/C_j are fixed at their measured values, while the measured values of C_j, C_{gnd} , and V_0 become $\beta_C C_j, \beta_C C_{gnd}$, and $\beta_V V_0$ in the calculations.

Figures 3 and 4 show that the theory including PAT fits both $\chi(f)$ and $\chi(V_0)$ with a single set of parameters for each pump. The measured parameters are given in the figure captions, and the scaling parameters are $\beta_C = 0.70$ and $\beta_V = 1.51$ for the 4-junction pump, and $\beta_C = 0.95$ and $\beta_V = 1.79$ for the 6-junction pump. From experimental uncertainties, we expect to find $\beta_C = 1 \pm 0.25$ and $\beta_V = 1 \pm 0.32$ (with approximately 95% confidence). The actual values of β_C are within or near the expected ranges, while the actual values of β_V are somewhat larger than expected. We attribute this to additional uncertainties involved in tuning the dc gate voltages to cancel the background charges, which are assumed to be zero in our calculations. Repeated measurements at a given f and V_0 over several weeks show that γ varies by as much as a factor of two from its average value, but it is difficult to convert these variations into quantitative uncertainties in β_C and β_V . Nevertheless, our results clearly demonstrate that the theoretical description of PAT is essentially correct.

It is of interest to identify the dominant PAT processes according to the theory. The calculations reveal that in both pumps the leakage is due almost entirely to single-junction ($m = 1$) processes. For the 4-junction pump at 60 GHz, the dominant processes involve a single tunneling event that brings the system over an energy barrier somewhat greater than $\hbar\omega$ with the assistance of two photons. In other words, Eq. (3) is dominated by a term with $m = 1$ and $n = 2$. This explains $\gamma \propto V_0^4$, since $J_n(x) \propto x^n$ for $x \ll 1$. For the 6-junction pump at 60 GHz, the dominant processes involve two tunneling events that each require a single photon. Both events are dominated by terms with $m = 1$ and $n = 1$ in Eq. (3). In this case, $\gamma \propto V_0^4$ results because the leakage rate involves the product of these two terms.

Our results show that PAT can be an important mechanism for leakage in electron pumps, and that an appropriate theory can accurately predict the leakage rate for a given pump and photon source. In the absence of applied microwaves, the leakage rate γ_b is much higher

than predicted by the standard theory that neglects PAT [5]: 10^5 and 10^{11} times higher for the 4- and 6-junction pumps, respectively. It is natural to ask whether this may be due to photons from a background noise source. In particular, it is important to estimate the effect of background charge noise with a $1/f$ spectrum since such noise is commonly observed in SET devices.

In two-junction SET electrometers with Al junctions, the input voltage noise measured at low frequencies, typically 0.01 Hz to 1000 Hz, generally has the form $S_V(f) = \alpha/f$ with $\alpha \sim (100 \text{ nV})^2$. This noise is believed to arise from an ensemble of charged defects moving among multiple states [18]. Such defects are also present in electron pumps, and since pumps and electrometers typically have similar capacitances, we expect that a comparable voltage noise appears across the pump junctions. We now make a key assumption: that the $1/f$ spectrum extends to ~ 100 GHz, so that it contains photons of sufficient energy to cause errors in our devices. This assumption would be difficult to justify for defects in equilibrium with the pump at 70 mK. However, because we observe that the low frequency electrometer noise decreases for at least a few weeks after cooldown [19], we believe that the defects are in fact slowly relaxing and may have an effective temperature of order 1 K or more. Although the standard equilibrium model of an ensemble of two-level systems that combine to give a $1/f$ spectrum [20] does not strictly apply in this case, the actual spectrum is unlikely to be dramatically different from $1/f$. We note that direct measurements of $1/f$ noise are limited to frequencies where the $1/f$ noise is larger than the white noise floor of the measurement system, whereas our measurement using the pump to “detect” the noise has no such limit.

We can evaluate the effect of the proposed $1/f$ noise using Eqs. (1) and (2). Taking $S_V(\varepsilon) = \alpha(h/\varepsilon)$ in Eq. (2), and the zero temperature rate $\Gamma_0(\Delta E) = \Delta E/e^2 R_j$ in Eq. (1), we find $\Gamma_e(\Delta E) = \pi\alpha/2R_j\Delta E$ (for single-photon processes with $\Delta E < 0$ and $|\Delta E| > k_B T$). We then use this rate to calculate the $1/f$ leakage rate $\gamma_{1/f}$ using the technique described in [5] that accounts for all possible tunneling sequences. When α is adjusted to give $\gamma_{1/f} = \gamma_b$, we find $\alpha = (7.7 \text{ nV})^2$ for the 4-junction pump and $\alpha = (26 \text{ nV})^2$ for the 6-junction pump. The fact that these values are within about an order of magnitude of the values typically measured in SET electrometers supports the hypothesis that $1/f$ noise persists to ~ 100 GHz and causes the background leakage rate in our experiments. It is important to note that devices other than electron pumps, particularly those requiring quantum coherence, such as the single-Cooper-pair transistor that has been proposed as a fundamental bit for quantum computing [21], may also be limited by this noise. Unless methods for eliminating $1/f$ noise from these devices can be devised, theoretical predictions of device performance should not neglect its effects.

In conclusion, environmental voltage sources can cause significant error rates in electron pumps. In our

experiment, photon-assisted leakage rates in 4- and 6-junction pumps are measured and compared to a theory that includes PAT. The theory matches the measured leakage rate as a function of both frequency and voltage with parameters that agree reasonably well with measured values. The background leakage rate in the absence of external microwaves is consistent with the hypothesis that leakage is driven by $1/f$ noise due to nonequilibrium fluctuating charges near the devices.

The authors acknowledge useful discussions about $1/f$ noise with Neil Zimmerman.

References

- [1] H. Grabert and M. H. Devoret, eds., *Single Charge Tunneling* (Plenum, New York, 1992).
- [2] H. Pothier *et al.*, *Europhys. Lett.* **17**, 249 (1992).
- [3] M. W. Keller, J. M. Martinis, N. M. Zimmerman, and A. H. Steinbach, *Appl. Phys. Lett.* **69**, 1804 (1996).
- [4] M. W. Keller, J. M. Martinis, and R. L. Kautz, *Phys. Rev. Lett.* **80**, 4530 (1998).
- [5] R. L. Kautz, M. W. Keller, and J. M. Martinis, *Phys. Rev. B* **60**, 8199 (1999).
- [6] M. H. Devoret *et al.*, *Phys. Rev. Lett.* **64**, 1824 (1990). S. M. Girvin *et al.*, *Phys. Rev. Lett.* **64**, 3183 (1990).
- [7] J. M. Martinis and M. Nahum, *Phys. Rev. B* **48**, 18316 (1993).
- [8] M. H. Pederson and M. Buttiker, *Phys. Rev. B* **58**, 12993 (1998) contains an extensive reference list.
- [9] J. M. Hergenrother *et al.*, *Phys. Rev. B* **51**, 9407 (1995). Y. Nakamura, C. D. Chen, and J. S. Tsai, *Czech. J. Phys.* **46**, 2301 (1996). R. J. Fitzgerald, J. M. Hergenrother, S. L. Pohlen, and M. Tinkham, *Phys. Rev. B* **57**, 9893 (1998).
- [10] A. A. Odintsov, *Sov. J. Low Temp. Phys.* **15**, 263 (1989). K. Flensberg, *et al.*, *Phys. Scripta* **T42**, 189 (1992). J. D. White and M. Wagner, *Phys. Rev. B* **48**, 2799 (1993). A. Hadicke and W. Krech, *Physica B* **193**, 265 (1994). I. A. Devyatov and K. K. Likharev, *Physica B* **194-196**, 1341 (1994).
- [11] M. W. Keller, A. L. Eichenberger, J. M. Martinis, and N. M. Zimmerman, *Science* **285**, 1706 (1999).
- [12] H. D. Jensen and J. M. Martinis, *Phys. Rev. B* **46**, 13407 (1992).
- [13] J. M. Martinis, M. Nahum, and H. D. Jensen, *Phys. Rev. Lett.* **72**, 904 (1994). M. W. Keller, J. M. Martinis, A. H. Steinbach, and N. M. Zimmerman, *IEEE Trans. Instrum. Meas.* **46**, 307 (1997).
- [14] M. L. Roukes *et al.*, *Phys. Rev. Lett.* **55**, 422 (1985).
- [15] A. H. Steinbach, J. M. Martinis, and M. H. Devoret, *Phys. Rev. Lett.* **76**, 3806 (1996).
- [16] In contrast to [4], the chips in this experiment do not track the mixing chamber temperature below 70 mK, possibly due to the use of a different sample mount. This is inconsequential to our measurements and conclusions.

- [17] H. D. Jensen and J. M. Martinis, *Physica B* **194-196**, 1255 (1994).
- [18] A. B. Zorin *et al.*, *Phys. Rev. B* **53**, 13682 (1996).
- [19] This behavior has not been carefully studied, but anecdotal reports indicate it is common in SET devices. A possibly analogous relaxation has been observed in amorphous silica, as described by J. Zimmerman and G. Weber, *Phys. Rev. Lett.* **46**, 661 (1981).
- [20] M. B. Weissman, *Rev. Mod. Phys.* **60**, 537 (1988).
- [21] A. Shnirman, G. Schon, and Z. Hermon, *Phys. Rev. Lett.* **79**, 2371 (1997). Y. Nakamura, Y. A. Pashkin, and J. S. Tsai, *Nature* **398**, 786 (1999).

Figure captions

Figure 1. (a) Schematic of the microwave circuit and a 4-junction pump. Tunnel junctions are represented by double-box symbols. The resistances which together comprise the 50Ω termination are $R_1 = 34 \Omega$, $R_2 = 31.5 \Omega$, $R_3 = 0.5 \Omega$, and $R_4 = 32 \Omega$. (b) Scanning electron microscope image of an actual chip. The Au/Au-Pd coplanar waveguide termination is the rectangular striped structure. The voltage taps to the pump and SQUID, as well as the locations of the pump and electrometer, are circled.

Figure 2. Electron temperature as a function of power in the termination at 32 GHz. The filled circles are experimental data and the solid line is $T_e^5 = T_{ph}^5 + (P_{out}/A)/\Sigma\Theta$, where $\Theta = 4.1 \times 10^4 \mu\text{m}^3$, $T_{ph} = 66 \text{ mK}$, $\Sigma = 1.4 \text{ nW}/\mu\text{m}^3\text{-K}^5$, and $A = 48 \text{ dB}$. The arrows indicate the range of power used while studying the photon-assisted leakage rate.

Figure 3. Photon-assisted leakage for a 4-junction pump in the hold mode. Main plot: $\gamma(f)$ for $V_0 = 21.9 \mu\text{V}$. Inset: $\gamma(V_0)$ for $f = 60 \text{ GHz}$. The filled circles are experimental data, the dashed lines are predictions based on Eq. (3) alone, and the solid lines include the background leakage rate γ_b . The measured parameters are $R_j = 460 \text{ k}\Omega$, $C_j = 0.20 \text{ fF}$, $C_{gnd} = 0.11 \text{ fF}$, $T_e = 67 \text{ mK}$, and $\gamma_b = 0.48 \text{ s}^{-1}$.

Figure 4. Photon-assisted leakage for a 6-junction pump in the hold mode. Main plot: $\gamma(f)$ for $V_0 = 18.4 \mu\text{V}$. Inset: $\gamma(V_0)$ for $f = 60 \text{ GHz}$. The filled circles are experimental data, the dashed lines are predictions based on Eq. (3) alone, and the solid lines include the background leakage rate γ_b . The measured parameters are $R_j = 670 \text{ k}\Omega$, $C_j = 0.20 \text{ fF}$, $C_{gnd} = 0.09 \text{ fF}$, $T_e = 67 \text{ mK}$, and $\gamma_b = 0.012 \text{ s}^{-1}$.

Fig. 1

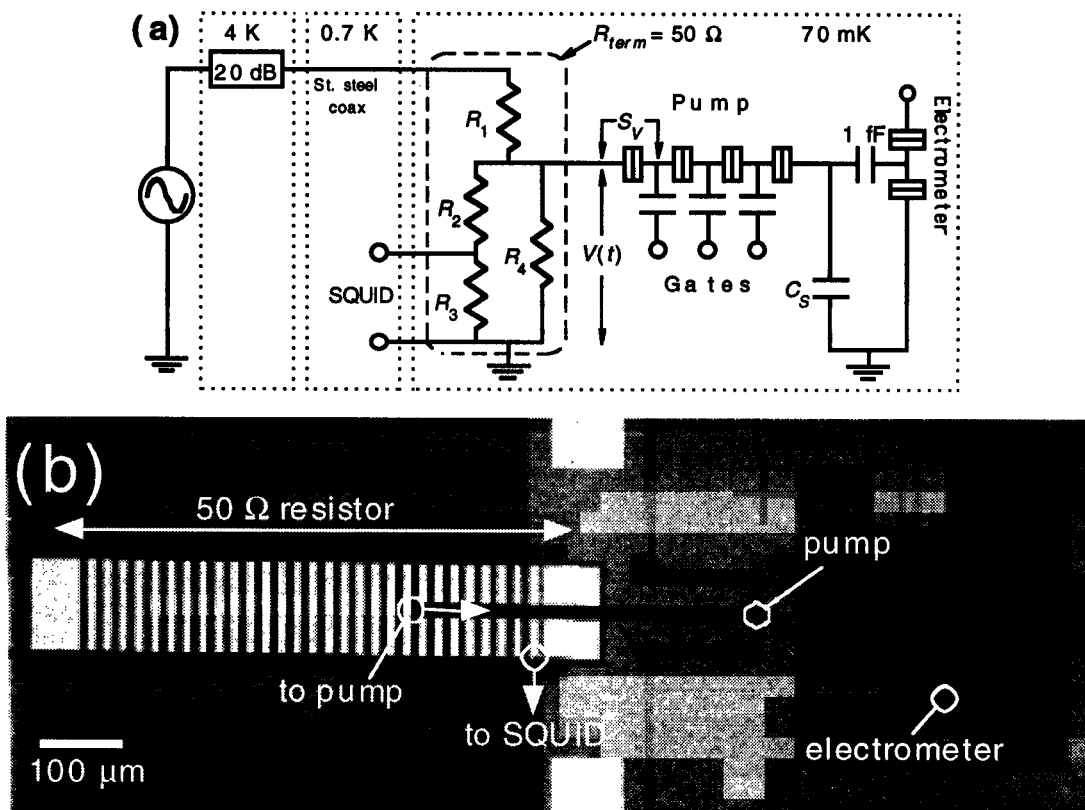


Fig. 2

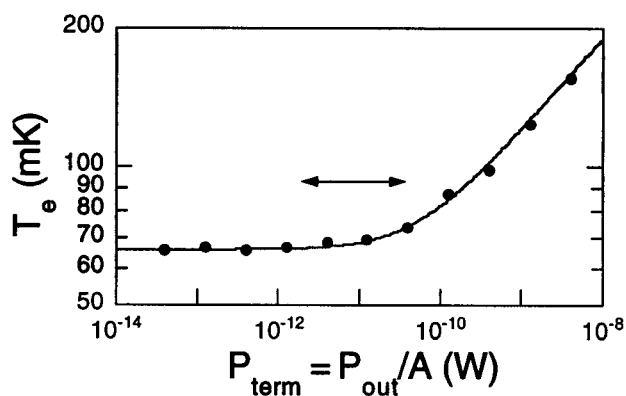


Fig. 3

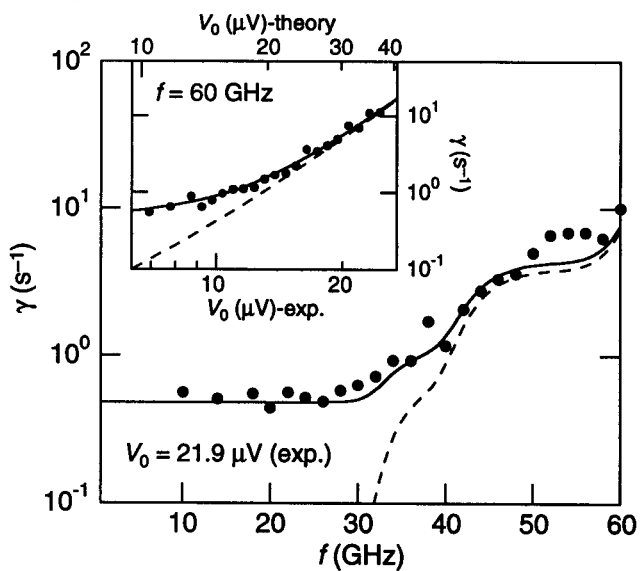


Fig. 4

